COMPUTER SIMULATION AND OPERATING CHARACTERISTICS OF A THREE–PHASE BRUSHLESS SYNCHRONOUS GENERATOR

Vlatko Čingoski - Mitsuru Mikami[†] - Kenji Inoue[‡] - Kazufumi Kaneda - Hideo Yamashita

This paper deals with numerical computation and simulation of the operating conditions of a three-phase brushless synchronous generator. A voltage driven nonlinear time-periodic finite element analysis is utilized to compute accurately the magnetic field distribution and the induced voltage and currents. The computation procedure is briefly addressed followed by the computed results and their comparison with experimental ones. The agreement between results is very good verifying the computational approach.

K e y w o r d s: Time-periodic nonlinear analysis, brushless synchronous generator, diode numerical modeling, rotating machines.

1 INTRODUCTION

Development of various electromagnetic devices with desired shape and operating parameters is usually very time consuming and laborious task. Besides the intensive mathematical calculation, the development of a prototype device and performing a set of experimentations must be done before the optimal design is achieved. With the increased usage of semiconductor devices and permanent needs for easy and reliable speed, torque, voltage and current on-line control, a typical 2-D or even 3-D finite element analysis is not enough adequate for design of the modern electrical machines. Therefore, recently with the increase of the computer performances and resources, designers are more interested how to accurately simulate the operating conditions of such devices instead of building a machine prototype and its testing. For such simulations, a new and more sophisticated methods and procedures must be employed [1].

This paper deals with numerical simulation and computation of operating characteristics of a 3-phase brushless synchronous generator [2]. To accurately predict and investigate the influence of various electrical parameters, and due to complexity of generator's configuration which includes several windings, rectifiers and transformer, several improvements in the ordinary finite element analysis must be accounted. In what follows, first, we briefly address the computation method and its mathematical background. Then, we present the numerically obtained results and their comparison with the measured ones in order to verify the correctness of our approach. Finally, we describe the simulation method and the obtained results for three-phase brushless synchronous generator, and give some final remarks and conclusions.

2 COMPUTATION METHOD

The configuration of the analyzed three-phase brushless generator, as can be seen from Fig. 1a is rather complex. The generator comprises four separate windings: the two-pole stator armature winding W_a and ten-pole excitation winding W_{es} on the stator side, and the two-pole source field winding W_f and ten-pole excitation winding W_{er} on the rotor side of the generator. The complexity of the circuit is further enhanced due to the existence of the rectifiers on both stator and rotor sides and a transformer VR. Therefore, in order to simulate the operating conditions of this genera-

Faculty of Engineering, Hiroshima University, 1-4-1 Kagamiyama, Higashihiroshima 739, Japan. Email: [vlatko, kin, yama]@eml.hiroshima-u.ac.jp

[†]Chugoku Electric Power Co., INC. - Hiroshima, Japan

[‡]Hiroshima Institute of Technology - Hiroshima, Japan

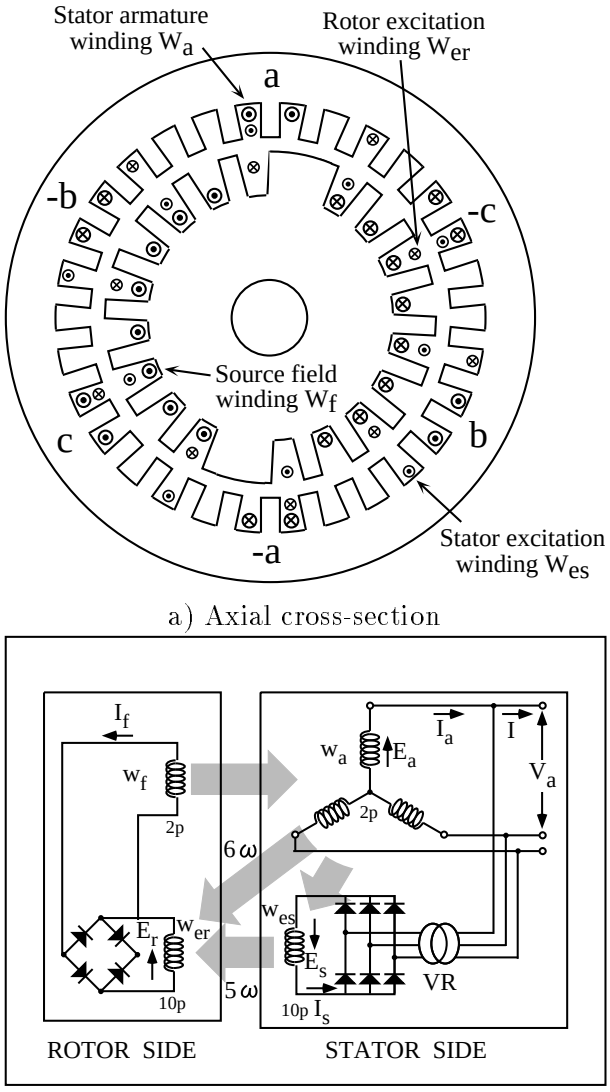

a) Axial cross-section

b) Electrical circuit

Fig. 1: Analyzed model of three-phase brushless synchronous generator.

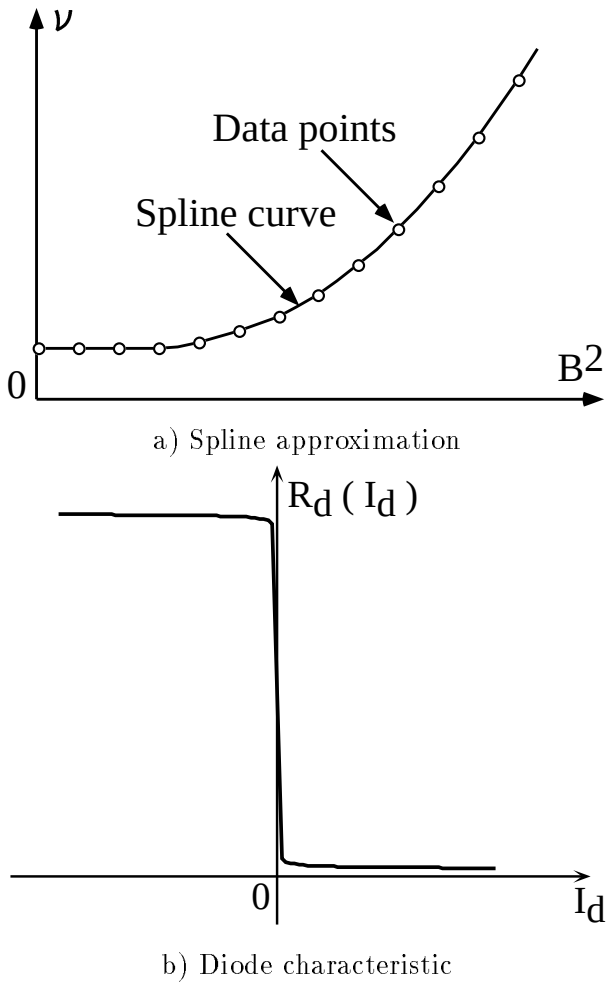

a) Spline approximation

b) Diode characteristic

Fig. 2: Approximation of the ν–B^2 and $R_d(I_d)$–I_d characteristics.

tor we developed a simulation method which posses the following features:

- Because the value of the currents are unknown in advance and they are strongly dependable on the circuit parameters, field distribution and operating conditions, the voltage driven finite element analysis must be performed. This analysis enables solving the magnetic field and electric circuit equations simultaneously.

- Nonlinear analysis must be perform due to the existence of saturated magnetic materials.

- Time-periodical step-by-step finite element method was employed in order to correctly evaluate the time–periodical characteristic of the generator's voltage and current changes due to its rotation [3].

- A method for numerical modeling of the diodes must be developed in order to successfully include them into the analysis.

- Computation and monitoring of the high frequency components of the voltage and currents must also be performed. These components are further emphasized in the analysis due to the existence of the rectifiers in the electric circuit.

2.1 Governing Equations

In the voltage source driven 2-D finite element analysis the governing system of equations which must be solved simultaneously are generated according to the Maxwell equations and the Second Kirchohoff Law

$$rot\,(\nu rot\mathtt{A}\,) = \mathtt{J}_{\mathtt{o}} - \sigma(\frac{\partial \mathtt{A}}{\partial t} + grad\phi)\,, \qquad (1)$$

$$\frac{\partial \Phi}{\partial t} + RI_0 + L\frac{\partial I_0}{\partial t} - V_0 = 0\,. \qquad (2)$$

where $\mathtt{A}$ is the magnetic vector potential, $\mathtt{J}_0$ is the source current density vector and ϕ is the electric scalar potential. Additionally, in Eq. (2), Φ stands for the total magnetic flux, I_0 and V_0 are the source current and supplied external voltage, while R and L are the resistance and inductance of the part of electric circuit which is not included inside the finite element analysis area. The coupling between Eq. (1) and Eq. (2) is enabled using the values of the source current intensity I_0 and its density vector $\mathtt{J}_0$, and the value of the total magnetic flux Φ given as

$$\mathtt{J}_0 = \frac{I_0}{S}\ \mathtt{n}\,, \qquad (3)$$

$$\Phi = N\int_{S_c} \mathtt{B}\cdot d\mathtt{S}_c\,, \qquad (4)$$

where $\mathtt{n}$ is the unit vector in the current flow direction, N is the number of turns per coil, S is the cross sectional area of the coil, and S_c is the area encircled by the coil and across which the magnetic flux passes through.

2.2 Nonlinear Modeling

As can be seen from Fig. 1, inside the analysis region, two strongly nonlinear elements exists: the nonlinear magnetic material and the rectifiers diodes. Because of the strongly nonlinear magnetic characteristics of the magnetic materials, in the analysis a nonlinear magnetic circuit must be considered, thus we utilized a traditional Newton-Raphson iteration process. For modeling of the magnetic characteristic ν–B^2 of the magnetic materials, a second order spline approximation was used utilizing previously available measured data as shown in Fig. 2a.

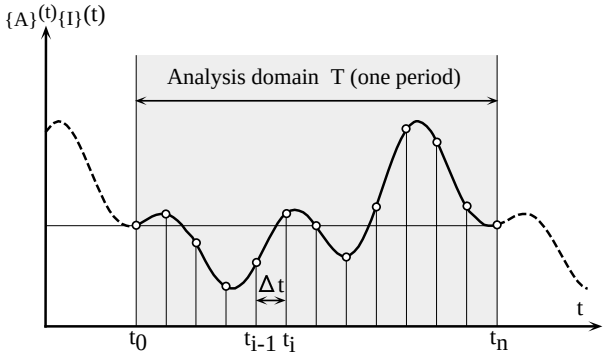

Fig. 3: Time periodical finite element analysis using step-by-step method.

For modeling of the nonlinear switching characteristic of the rectifiers diodes, shown in Fig. 2b, we must model the resistance of the diodes according to the current changes. This modeling was done according to the following empirical equations

$$R_d(I_d) = \begin{cases} \frac{1}{\sqrt{100(I_d+4.0\times10^{-10})}} & (I_d \geq 0) \\ \frac{-1}{\sqrt{-100(I_d-4.0\times10^{-10})}} + 10000 & (I_d < 0) \end{cases} \qquad (5)$$

2.3 Time-periodical FEA

Another important issue is the modeling of the first derivatives of the current and magnetic vector potential. Due to their periodical but non-sinusoidal characteristic they can not be simply modeled using complex representation, but a time discretization must be employed. In the analysis we employed the step-by-step method schematically shown in Fig. 3. This method enables representation of the first derivative of any time-changing variable, e.g. the current, at each time step t as a function of its value at time $t - \Delta t$

$$\frac{\partial I_0^{(t)}}{\partial t} = \frac{I_0^{(t)} - I_0^{(t-\Delta t)}}{\Delta t} \qquad (6)$$

where Δt is the computation time step.

It is very important to notice that as shown in Fig. 3 one of the necessity conditions is that the values of the unknown variable coincide at the terminal points of the analysis time domain which is usually equal to one time period. This condition enables generation of the following system of algebraic equations

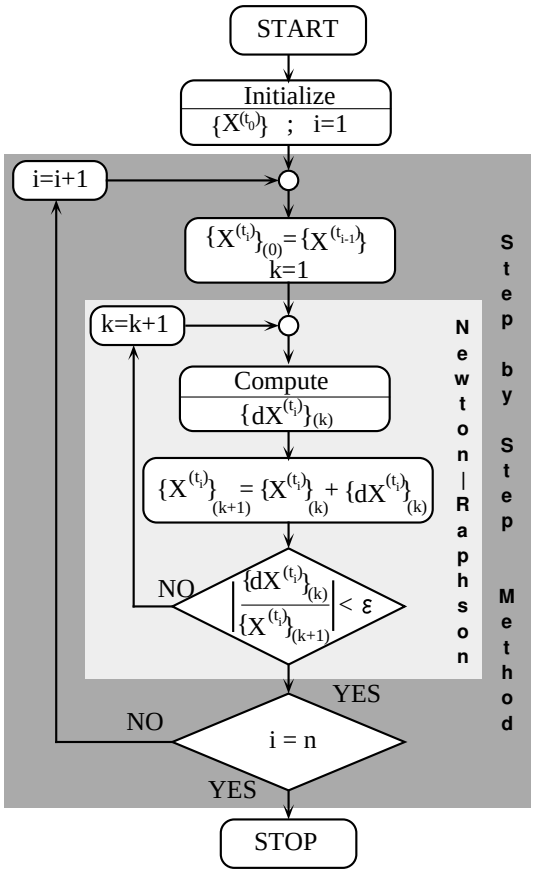

Fig. 4: Nonlinear step-by-step finite element analysis.

$$\begin{Bmatrix}\{0\}\\ \{0\}\end{Bmatrix} = \begin{bmatrix}[K]^{(t)}+[T] & [S]\\ [S]^T & [Z_R]^{(t)}+[Z_X]\end{bmatrix}\begin{Bmatrix}\{A\}^{(t)}\\ \{I\}^{(t)}\end{Bmatrix} - \begin{bmatrix}[T] & [0]\\ [S]^T & [Z_X]\end{bmatrix}\begin{Bmatrix}\{A\}^{(t-\Delta t)}\\ \{I\}^{(t-\Delta t)}\end{Bmatrix} - \begin{Bmatrix}\{0\}\\ \{V\}^{(t)}\end{Bmatrix} \quad (7)$$

Finally, according to the periodical symmetry of the model and its rotation inside the magnetic field the system of linear equations (7), must be transformed using periodical boundary conditions. The generated algebraic system of equations could be solved by any direct or iterative method such as $ICCG$ method resulting with the desired values for magnetic vector potential and current values at each time step, respectively.

The simplified algorithm for the nonlinear step-by-step finite element analysis procedure utilized in this paper is shown in Fig. 4.

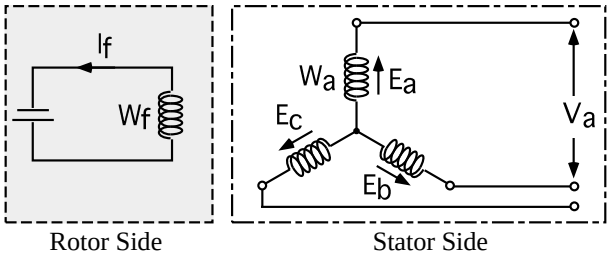

Fig. 5: Electric circuit for no-load characteristic simulation.

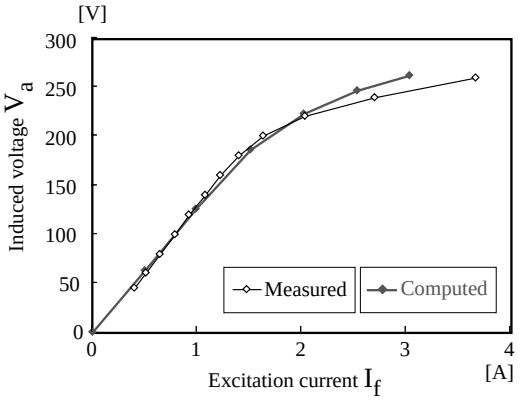

Fig. 6: Computer simulated no-load characteristic of the generator.

3 SIMULATION RESULTS

3.1 No-load Characteristics

The electric circuit developed for simulation of the no-load characteristic is given in Fig. 5, while the obtained no-load characteristic is given in Fig. 6, together with the experimental data obtained by performing measurements on the model generator. Actually, since the magnetic characteristic of the material was unknown, these measured data were used for modeling of the B–H magnetic curve, i.e. the ν–B^2 curve. As can be seen from Fig. 6 computed results are in very good agreement with the measured ones almost for the entire working area. The small discrepancy can be observed only for large values of the excitation current, which we believe, is the result of the large saturation of magnetic materials for large amounts of source currents on the model generator and which was difficult to be included

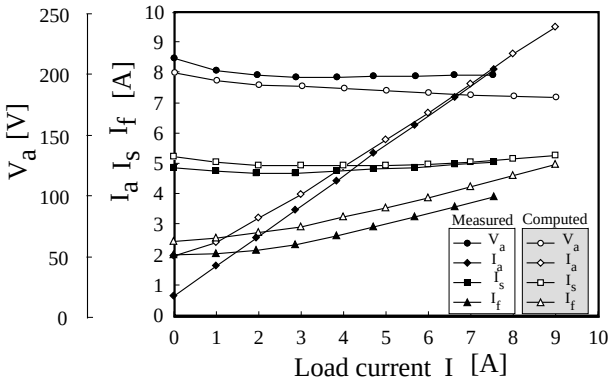

Fig. 7: Computer simulated load characteristics of the generator.

into computer simulation.

3.2 Load Characteristics

For simulation of the load characteristics of the analyzed synchronous generator, the electric circuit shown in Fig. 1b was utilized. As can be seen, the couplings among the stator and rotor windings for this circuit are strong, and the existence of diodes and transformer VR makes the computer simulation extremely complex.

Several parameters of the generator were monitoring during simulation of the load condition, among them, the time changes and the maximum induced voltage V_a at generator's terminals, the maximum value of the source field current I_f and the values of excitation currents I_s and I_r on stator and rotor side, respectively. Figure 7 shows the obtained results of the computer simulation using time step of one electrical degree. In the same figure, for comparison the measured values are also plotted. As can be seen, computed result are in very good agreement with measured ones for almost entire working area. However, small discrepancy between measured and computed results can be still observed especially for small values of the load current I, which discrepancy is particularly emphasized for armature current I_a of the generator. We believe that this is result of the modeling method for the transformer VR and neglecting its magnetic losses.

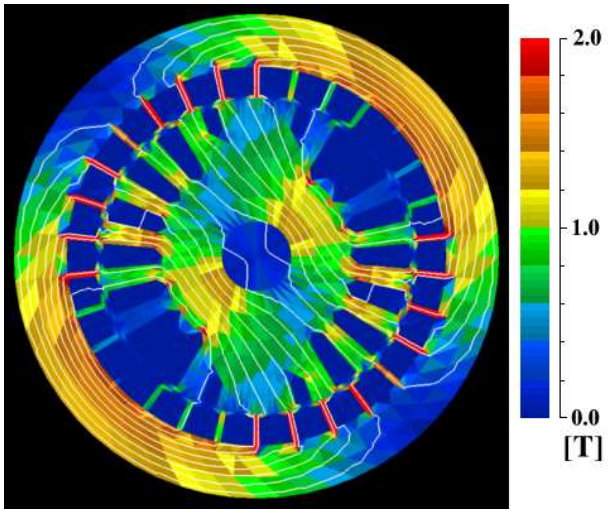

Fig. 8: Gray-scale still image for the magnetic flux distribution.

Table I: Computational cost per analysis.

Total number of unknowns (Points + Sources) × Time Steps	Computation time
(1635 + 10) × 360 = 592200	about 12 hours

In Fig. 8, the computed intensity distribution of magnetic flux density `B` is shown together with flux lines at one particular time step. Additionally, in Fig. 9 time changes of the induced voltage of the analyzed generator for all three phases are presented. From this figure it is readily visible that the induced voltage exhibits ripples which are the result of the neglecting the skewing structure of the rotor. This should be priority in our future research.

Finally, Table I shows the number of unknowns and the total computation time for one analysis with the above described nonlinear time-periodical finite element analysis. As can be seen, although the number of unknowns is rather large, the computation time of approximately 12 hours is still acceptable for such a complex analysis.

4 CONCLUSION

We presented a method for numerical computation and simulation of three-phase brushless synchronous generator under operating conditions. Using voltage driven 2D time-periodic

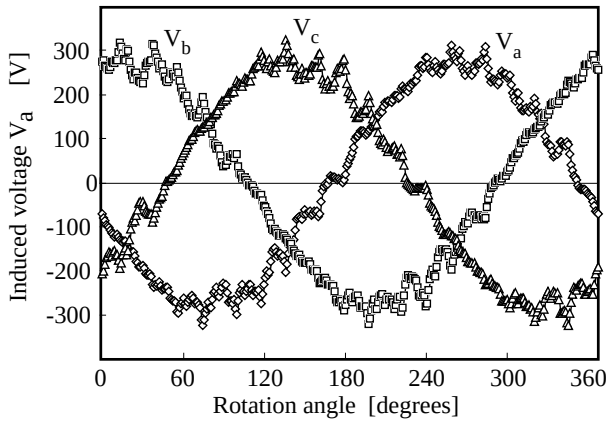

Fig. 9: Time-periodical changes of induced voltage V_a, V_b and V_c.

nonlinear finite element analysis, the magnetic field distribution and the induced voltage and currents were computed accurately. For modeling of the diode characteristic a simple and fast emprical equations were used, while the magnetic charactersitic was modeled using second order spline approximation. The computational approach was verified using exeperimental results obtained from the test model of brushless synchronous generator. The achieved agreement between experimental results and computed results was very good.

References

[1] T. Nakata, et al.: "Direct Finite Element Analysis of Flux and Current Distributions under Specified Conditions,"*IEEE Transaction on Magnetics*, MAG-18, No.2, pp.325, 1988.

[2] K. Inoue, et al.: "Brushless Self-Excited Three-Phase Synchronous Generator without Exciter,"*Transaction on IEE of Japan*, D.112, No.6, pp.596, 1992. (in Japanese)

[3] T. Hara, et al.: "Field Analysis of Corona Shield Region in High Voltage Rotating Machines by Time-Periodic Finite Element Method: I. Numerical Calculation Method, "*Transaction on IEE of Japan*, D.102, No.7, pp.423, 1982. (in Japanese)

Vlatko Čingoski (Ass.Prof., D.Eng.), born in Ohrid, Macedonia, in 1962. He received the B.E. and M.E. degrees in electrical engineering from the "Sts. Cyril & Methodius"University, Skopje, Macedonia, in 1986 and 1990, respectively, and Doctor of Engineering degree in 1996 from Hiroshima University, Hiroshima, Japan. Since 1996 he has been an Assistant Professor at Electric Machinery Laboratory, Faculty of Engineering, Hiroshima University.

Mitsuru Mikami (M.E.), born in Hiroshima, Japan, in 1972. He received the B.E. and M.E. degrees in electrical engineering from Hiroshima University, Hiroshima, Japan, in 1995 and 1997, respectively. Since April 1997 he works as a electric engineer in The Chugoku Electric Power Co., Inc., Hiroshima, Japan.

Kenji Inoue (Asc.Prof.), born in Hiroshima, Japan in 1941. He received the B.E. degree in electrical engineering from Hiroshima Institute of Technology, Hiroshima, Japan in 1967. Since 1989, he has been an Associate Professor at Hiroshima Institute of Technology, Hiroshima, Japan.

Kazufumi Kaneda (Asc.Prof., D.Eng.), born in Totori, Japan, in 1959. He received the B.E., M.E., and Doctor of Engineering degrees from Hiroshima University, Japan, in 1982, 1984, and 1991, respectively. Since 1995, he has been an Associate Professor at Electric Machinery Laboratory, Faculty of Engineering, Hiroshima University.

Hideo Yamashita (Prof., D.Eng.), born in Kure, Japan, in 1941. He received the B.E. and M.E. degrees in electrical engineering from Hiroshima University, Hiroshima, Japan, in 1964 and 1968, and Doctor of Engineering degree in 1977 from Waseda University, Tokyo, Japan. Since 1992 he has been a Professor at Electric Machinery Laboratory, Faculty of Engineering, Hiroshima University.